Thermal oxidation of aromatic epoxy-diamine networks

Justine Delozanne [a, b], Nancy Desgardin [b], Nicolas Cuvillier [b], Emmanuel Richaud [a, *]

[a] Laboratoire PIMM, Arts et Metiers ParisTech, CNRS, Cnam, 151 boulevard de l'Hôpital, 75013, Paris, France
[b] SAFRAN Composites, 33 avenue de la Gare, 91760, Itteville, France

A B S T R A C T

The thermal oxidation of DGEBA-DDS (bisphenol A diglycidyl ether + 4,4′-diaminodiphenyl sulfone) and TGMDA-DDS (4,4′-methylenebis(N,N-diglycidylaniline) + 4,4′-diaminodiphenyl sulfone) was performed at 80, 120, and 200 °C and was monitored by FTIR. Oxidation was shown to generate amides and carbonyls. Comparisons were done with model systems displaying some common reactive groups, which highlighted the predominating role of methylene in α position of ether in DGEBA-DDS and methylene in α position of nitrogen hold by TGMDA in TGMDA-DDS. The participation of CH_2 in α position of DDS hardener group seems to depend on the temperature and decrease when lowering it. The oxidation of such complex systems must hence be described by a co-oxidation model where each kind of reactive sites is described by its own set of kinetic constants.

Keywords:
Epoxy-diamine
Thermal oxidation
FTIR

1. Introduction

Thermal oxidation of epoxies is documented to induce chain scissions [1,2] and later volatile compounds [3,4]. The subsequent mass loss results in the appearance of cracks favoring the access of oxygen to deeper layers [5]. In the field of epoxy adhesives used at high temperatures, mass loss seems correlated with the drop of adhesive strength [6]. In a recent work on titanium/epoxy/titanium bonded assemblies, microscopic analyses lead us to propose that thermal oxidation induced a cohesive failure of the epoxy-adhesive [7]. Such mechanisms of embrittlement seem to originate from the depletion of the β relaxation associated to plasticity and toughness in epoxy/diamine networks [8] i.e. from the radical attack of hydroxypropylethers groups.

It is hence crucial to understand the reactivity of hydroxypropylethers for predicting lifetime of epoxy networks. However, one of the main difficulties is that epoxy-diamine networks are insoluble and can only be analyzed by FTIR at low conversion degrees of oxidation. Another difficulty is linked to the structural complexity of epoxy-diamine networks family, which is actually constituted by a wide number of prepolymer hardener pairs, where several sites are likely to participate to the oxidation process [9–11]. The glass transition of networks ranges from less than 100 °C to more than 200 °C [2,12,13] so that a supplementary level of complexity linked to the effect of macromolecular mobility might complicate the comparison of data obtained in glassy state or rubbery one.

DGEBA-DDS and TGMDA-DDS appear as ideal cases since hydroxypropylethers are possibly the only reactive site. Moreover, their oxidation at temperatures below 200 °C can be compared only in terms of reactivity since both networks are in glassy state (and above their β relaxation) in this temperature range. However, few papers deal with their oxidation at molecular level. Most of them address either the case of high temperature thermal degradation of TGMDA-DDS (T > 200 °C where mechanisms would be initiated by water elimination in secondary alcohol groups i.e. -O-CH_2-CHOH-CH_2-N< → -O-CH_2-CH=CH_2-N< + H_2O [14–16]) or photo-oxidation of DGEBA-DDS [17,18] at moderate temperature. Determining the thermal oxidation mechanism of aromatic networks in the maximal use temperatures of airplanes (~120 °C) remains thus for us an open task.

The aim of this paper is therefore to compare the reactivity of DGEBA-DDS and TGMDA-DDS in thermal degradation at moderate temperature and understand the nature of reactive sites, so as to answer to the following questions:

- which sites are the more oxidizable in hydroxypropylethers?
- what is the most probable mechanism (in terms of degradation kinetics)?
- what is the role of chemical environment on the oxidation of hydroxypropylethers?

Since all oxidation products appear in a relatively narrow wavenumber range, we will also study the degradation of model systems with common reactive sites so as to better understand the

* Corresponding author.
E-mail address: emmanuel.richaud@ensam.eu (E. Richaud).

degradation of TGMDA-DDS and DGEBA-DDS.

The answers of those questions will help to conclude on the reliability of the hypothesis according to which the thermal oxidation of aromatic epoxy networks can be modeled by considering the isoreactivity of each site present in the network [19–21].

2. Experimental

2.1. Materials

Two epoxy-diamine systems were based on chemicals presented in Fig. 1:

- DGEBA (DER 330, CAS 25058-38-6) supplied by Dow ($M = 340\ g\ mol^{-1}$)
- TGMDA (ARALDITE MY721 CH, CAS 28768-32-3) supplied by Huntsman ($M = 422\ g\ mol^{-1}$)
- DDS (ARADUR 976-1 NL, CAS 80-08-0) supplied by Huntsman ($M = 248\ g\ mol^{-1}$)

Some comparisons were performed with DGEBA and TGMDA in their unreacted form.

A linear phenoxy resin (denoted by PKHJ - CAS: 25068-38-6 - ref 181196-250G from Sigma Aldrich) was also studied. This latter was supplied as pellets which were pressed at 200 °C during 60 s using a Gibritte press so as to obtain about 35 μm thin films.

The in-situ DSC (Q10 apparatus — TA Instruments) curing of TGMDA-DDS and DGEBA-DDS was studied by heating samples from −70 °C to 300 °C at a 10 °C min^{-1} rate under 50 ml min^{-1} nitrogen flow (see Fig. 2 for TGMDA-DDS). The measured characteristics (temperature of maximal heat release T_{max}, onset temperature T_{onset}, curing enthalpy ΔH) are gathered in Table 1.

DGEBA-DDS and TGMDA-DDS were hence cured at 150 °C during 3 h under vacuum so as to get about 30 μm thick films in which the Diffusion Limited Oxidation effects [22] can be neglected. TGMDA-DDS and DGEBA-DDS were then post cured respectively 1 h at 180 °C and 1 h at 200 °C under nitrogen (so as to limit the pre-oxidation). The degree of cure (very close to 100%) was checked from the disappearance of any residual exotherm.

2.2. Exposure conditions

Thermal ageing of 35 μm films was performed in ventilated ovens (System Climatic Service) at 80, 120, and 200 °C under air.

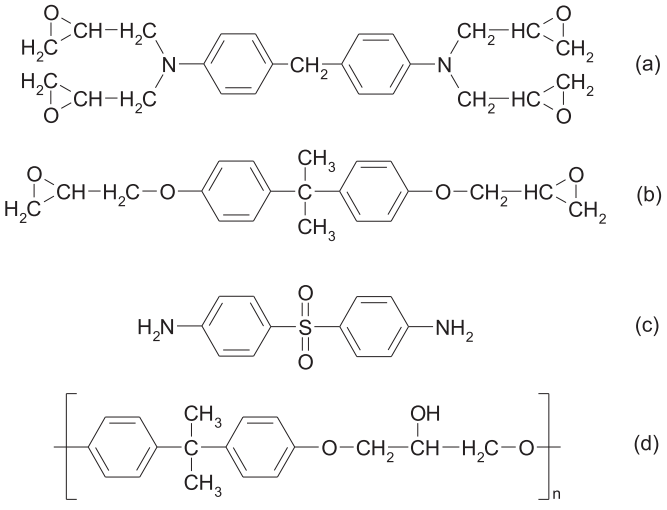

Fig. 1. Structure of monomers and model systems under study: TGMDA (a), DGEBA (b), DDS (c), PKHJ (d).

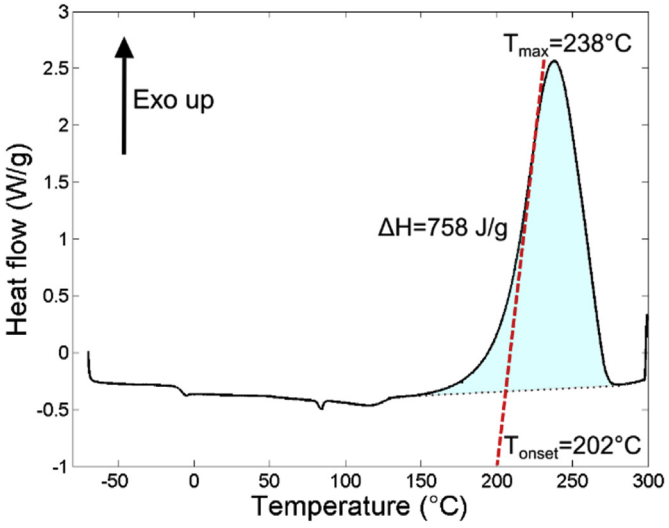

Fig. 2. Curing thermogram of TGMDA-DDS.

2.3. Characterization

FTIR spectroscopy was used in transmission mode on thin DGEBA-DDS, TGMDA-DDS and PKHJ films using a Frontier apparatus (PerkinElmer) by averaging 16 scans in the 400-4000 cm^{-1} wavenumber range at a 4 cm^{-1} resolution. Absorbances were measured by subtracting the baseline value and were then converted in concentration using Beer-Lambert law:

$$A_\lambda = \varepsilon_\lambda \times l \times c \quad (1)$$

where A_λ is the absorbance, l the thickness of the film (expressed in cm), c the concentration (in mol l^{-1}) and ε_λ the molar absorptivity at the considered wavenumber (in l mol^{-1} cm^{-1}). Concentrations of oxidation products were thus assessed using molar absorptivity values equal to 500 l mol^{-1} cm^{-1} for carbonyls at 1765 cm^{-1} in PKHJ (estimated from phenyl acetate — see Appendix 1), 680 l mol^{-1} cm^{-1} for carboxylic acids at 1730 cm^{-1} in TGMDA-DDS [23] and 470 l mol^{-1} cm^{-1} for amides at 1675 cm^{-1} [10] (NB: the nature of the products will be justified later).

Some comparisons were performed with the oxidation of TGMDA and DGEBA monomers. A single drop of monomer solution in THF was casted on KBr plates and evaporated. The thickness was assessed from the aryl absorbance (1614 cm^{-1}) with $\varepsilon = 320$ l mol^{-1} cm^{-1} for TGMDA (this value was estimated from a single calibration in a 12 μm thin cell).

The analysis of wavelength region ranging from 1600 to 1800 cm^{-1} is tricky because of the overlapping of several absorptions due to various stable products. The broad bands were hence deconvoluted for a better scrutiny. The deconvoluted peaks were supposed to be gaussian with maximal absorption, wavenumber of maximal absorbance and width at middle height as fitting parameters.

3. Results

3.1. Formation of stable products epoxy amine networks and their model systems

3.1.1. DGEBA-DDS

Spectra of DGEBA-DDS samples after varying exposure times at 120 °C are overlapped in Fig. 3 which calls for the following comments:

Table 1
Results of DSC curing.

Systems	Curing exotherm ΔH (J g^{-1})	Onset temperature T_{onset} (°C)	Temperature of maximal exothermicity T_{max} (°C)
TGMDA-DDS	758	202	238
DGEBA-DDS	300	187	230

- No significant changes are observed for signals due to aromatic rings (1595, 1509 and 1362 cm^{-1}).
- The main changes are observed in the 1600-1800 cm^{-1} wavenumber range with maxima at 1682, 1730 and 1767 cm^{-1} respectively ascribed to amides, carbonyls and formates. Absorbance for formates was checked from model compounds (see Appendix 1). The origin of each product will be commented in detail later. The 1760 cm^{-1} band was then considered as exclusively due to formates and exploited using $\varepsilon = 500$ l mol^{-1} cm^{-1} whereas our interpretation of mechanisms (see 'Discussion') lead us to attribute 1725 cm^{-1} to carboxylic acids (with a 680 l mol^{-1} absorptivity).
- A slow decrease is observed in the hydroxyl region (3500-3300 cm^{-1}) suggesting that water elimination is negligible here. This will receive a more thorough attention in the following.
- A decrease is observed for the absorbance at 1039 cm^{-1} (Ar-O-CH_2- [24]) and for 1109 cm^{-1} one (secondary alcohol [25]). According to Fig. 4, the decrease of 1039 cm^{-1} absorbance is faster than 1109 one suggesting that methylene group in α position of ether is more sensitive to radical oxidation than methine group in α position of alcohol.
- According to Fig. 5, the decrease of 2871 and 2930 cm^{-1} absorbances (ascribed to methylenes [17]) seems faster than 2966 cm^{-1} one (ascribed to CH_3 of DGEBA) as shown in Fig. 5. According to the case of polycarbonate photo-oxidation [26,27] or DGEBA-diamine [28], isopropylidene groups could yield acetophenones (1684 cm^{-1}). The absence of well-defined maxima at this wavenumber (Fig. 3) together with the slow decrease of the absorbance at 2966 cm^{-1} (C-CH_3) demonstrates the higher stability of isopropylidene groups compared to the C-H at vicinity of heteroatoms.

The region corresponding to amides and carbonyls (1600-1800 cm^{-1}) is complex to analyze because of overlapping of several absorbances. The broad band was deconvoluted to better highlight the main oxidation stable products [29] (see Fig. 3c and 3d). It is observed that:

- formates (1765 cm^{-1}) are formed as soon as the beginning of exposure.
- carbonyls predominate over amides at short exposure times (about 500 h) whereas those later would predominate at relatively long exposure times (>4000 h).

For ageing at 200 °C, formates and other carbonyls are also formed but the formation of amides is here observed to predominate even at short exposure times (Fig. 6).

3.1.2. TGMDA-DDS

Fig. 7 displays spectra for TGMDA-DDS after several ageing

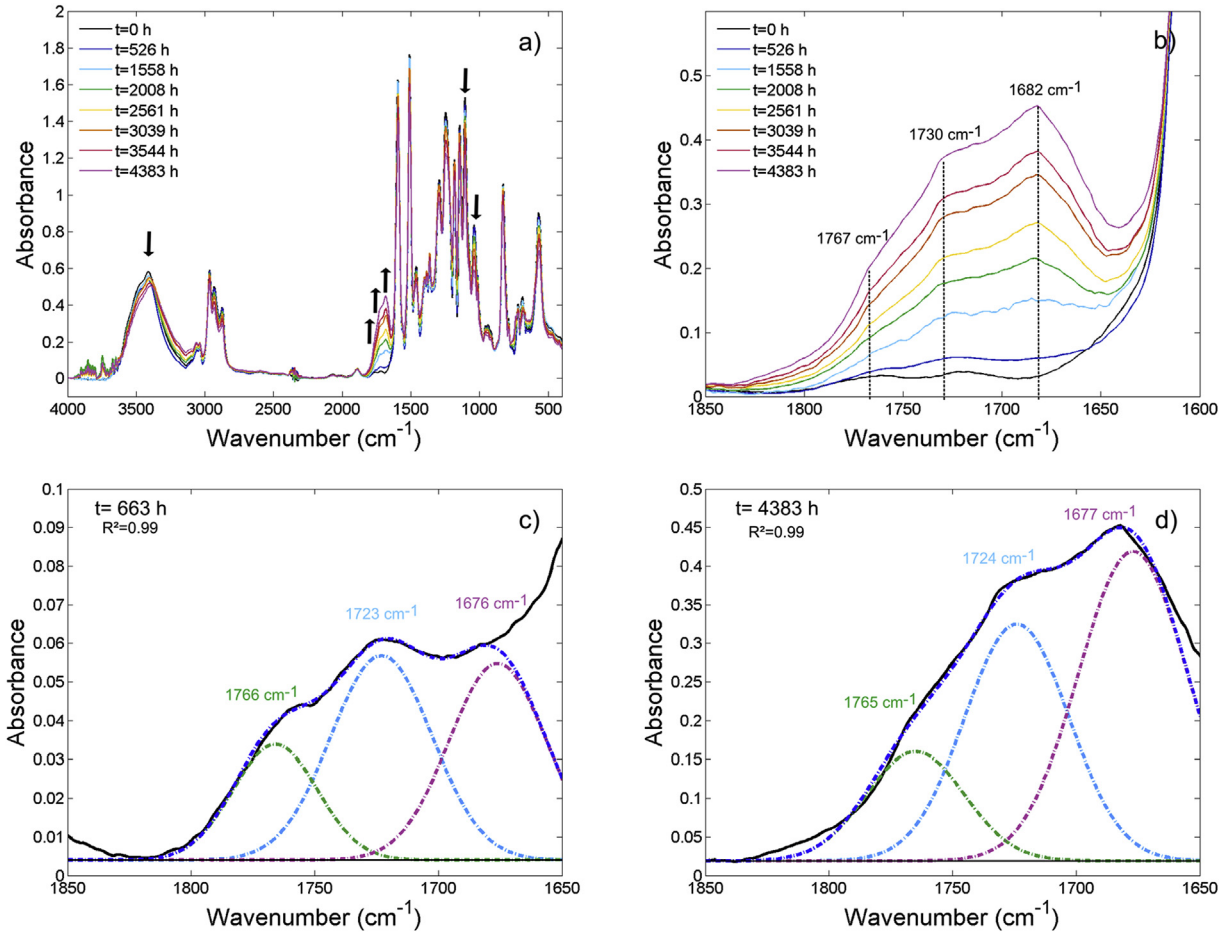

Fig. 3. FTIR spectra for DGEBA-DDS thermally oxidized at 120 °C: full scale spectra (a), carbonyl region (b), deconvolution after 663 h (c) and 4383 h (d) of thermal ageing.

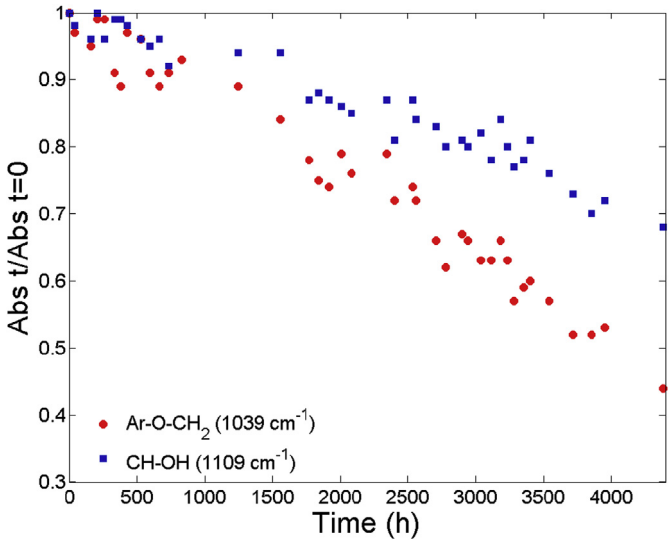

Fig. 4. Relative decrease of -Ar-O-CH_2- and >CH-OH absorbance for DGEBA-DDS thermally oxidized at 120 °C.

durations at 120 °C. It calls for the following comments:

- The main change is the rapid formation of amides absorbing at 1675 cm^{-1} together with a secondary peak at 1723 cm^{-1} corresponding to several possible carbonyl groups (carboxylic acids, ketones …) as discussed later. The amide absorbance is shifted at higher exposure times suggesting changes in its chemical surrounding. This peak is actually complex but a mechanistic discussion lead us to consider it is in great part due to carboxylic acids which were quantified using $\varepsilon = 680\ l\ mol^{-1}\ cm^{-1}$.
- Deconvolutions (Fig. 7c and d) suggest the presence of absorbances at 1645 and 1740 cm^{-1} that remain however negligible compared to 1675 and 1723 cm^{-1} ones at long exposure times (4500 h).
- The absorbances for methylenes visible at 2910 and 1460 cm^{-1} [16] are observed to decrease. It is however difficult at this stage to conclude which kind of methylene (>CH_2 between aromatic rings of TGMDA or in α position of nitrogens) is the most degraded.

As developed in the following, the amide build-up at 1675 cm^{-1} is obviously higher for TGMDA-DDS than for DGEBA-DDS. It means that methylene in α position of the nitrogen atom belonging to TGMDA monomer are more sensitive than methylene group in α position of DDS hardener at least at moderate temperature (such as 120 °C).

According to literature [14–16], the degradation mechanisms of TGMDA-DDS and DGEBA-DDS would involve a preliminary water elimination reaction followed by the oxidation of the allylic methylene groups in the generated >N-CH_2-CH=CH-N< groups. The occurrence of this reaction was tentatively assessed from the changes of the >CH-OH and = C-H stretching (Fig. 8). The absence of significant changes even at 200 °C and 120 °C in the timescale where amides are produced leads us to neglect, in a first approach, this reaction in the following of the paper.

3.1.3. TGMDA monomers

To better understand the origin of amides buildup, TGMDA monomer was aged at 120 °C (Fig. 9). It is shown that:

- Oxidation products are very similar to those observed in TGMDA-DDS confirming the predominating role of methylene at the vicinity of nitrogen hold by TGMDA.
- The amides formation is very fast which confirms the instability of this last methylene group. As quantified more precisely later, its predominance over carbonyls one also indicates that methylene in α position of nitrogens are less stable than the oxirane rings or the CH_2 in α position of ethers (apart if the carbonyls formed from those later are volatile products).
- The product formed at 1645 cm^{-1} could correspond to methyl quinone [27] formed from the oxidation of methylene group located between aromatic rings. However, its low quantity suggests that this group is quite stable in TGMDA and TGMDA-DDS (Figs. 7 and 10) and possibly more than the hydroxypropylether moiety.

3.1.4. PKHJ and DGEBA monomers

In order to understand the origin of formates (1765 cm^{-1}) and carboxylic acids or ketones (about 1730 cm^{-1}) when the substrate does not hold nitrogen atom, a linear phenoxy polymer (PKHJ) and DGEBA monomer were thermally aged so as to compare the reactivity of isopropylidene, CH_2 in α position of ether and CH in α position of alcohol. Results are presented in Figs. 10–12.

Identically to DGEBA-DDS, a formate (absorbing at 1760 cm^{-1}) is generated, together with other kinds of carbonyls absorbing at 1727 cm^{-1} (Fig. 10). Firstly, a part of this absorbance is due to the formates (see FTIR spectra in Appendix 1). The other part might come from the degradation of:

- methyl groups, but this seems negligible here since the peaks at 2966 cm^{-1} remain stable (Fig. 11) and there is no evidence for acetophenone coming from the isopropylidene degradation (absorbing at about 1684 cm^{-1}).
- methines in α position of alcohol (>CH-OH) which seems also a minor route since the 1109 cm^{-1} band remains unchanged.
- formates themselves as it will be proposed in the 'Discussion' section (Scheme 1).

However, it seems reasonable to consider, in a first approach, that formates are the predominating species formed in PKHJ oxidation.

The comparison with oxidation of DGEBA monomer (Fig. 12) shows.

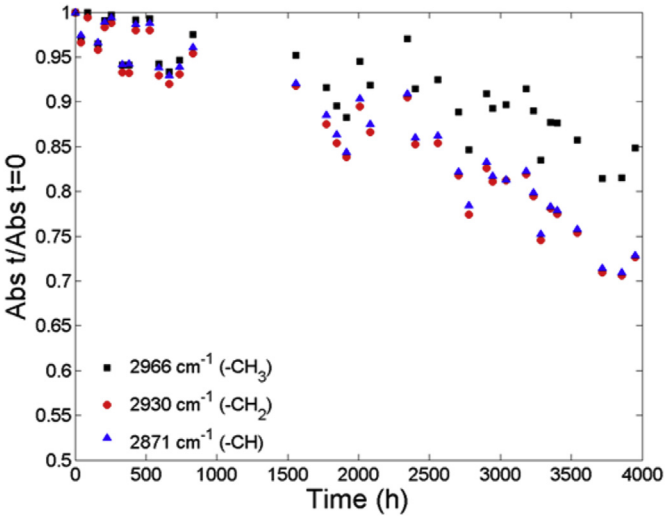

Fig. 5. Relative decrease of -CH_3, -CH_2- and >CH- absorbance for DGEBA-DDS thermally oxidized at 120 °C.

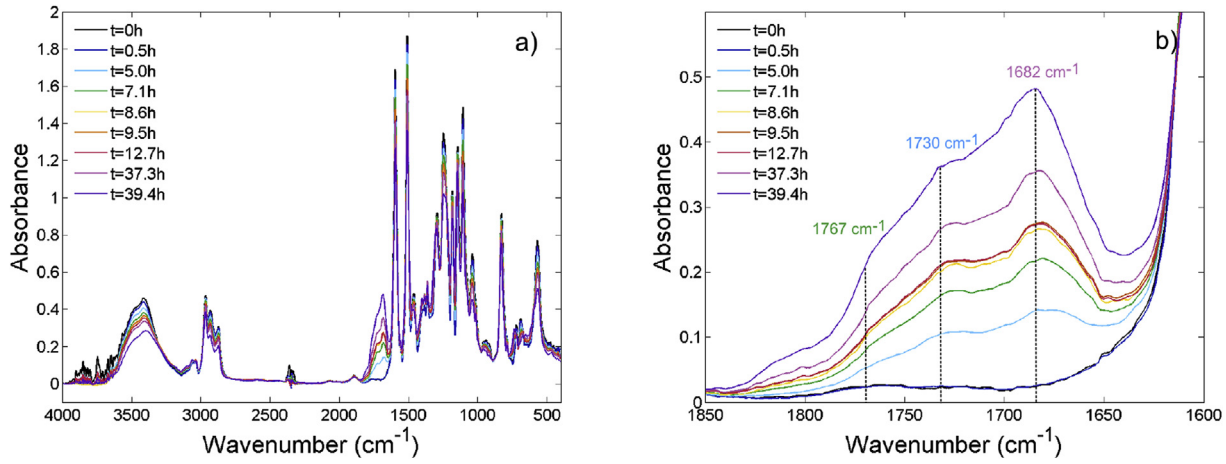

Fig. 6. FTIR spectra for DGEBA-DDS thermally oxidized at 200 °C: full scale spectra (a) and carbonyl region (b).

- the appearance of an absorbance at 1760 cm^{-1}, confirming its link with the -Ar-O-CH_2- group, the prominent role of which being confirmed since the formate predominates both in PHKJ and DGEBA in the earliest times of oxidation. Identically to DGEBA-DDS, formates will be considered as the key oxidation products and quantified using $\varepsilon = 500\,l\,mol^{-1}\,cm^{-1}$.
- a strong absorbance at 1727 cm^{-1} suggesting that oxirane rings are much more reactive than secondary alcohols.

3.2. Kinetics of buildup of stable products

Concentrations in amides and carbonyls in TGMDA-DDS, DGEBA-DDS, PKHJ and TGMDA were estimated from Eq. (1). Carbonyl absorbance based on 1730 cm^{-1} absorbance actually is quite intricate:

- formates formed at 1765 cm^{-1} contribute to this peak (see Appendix).

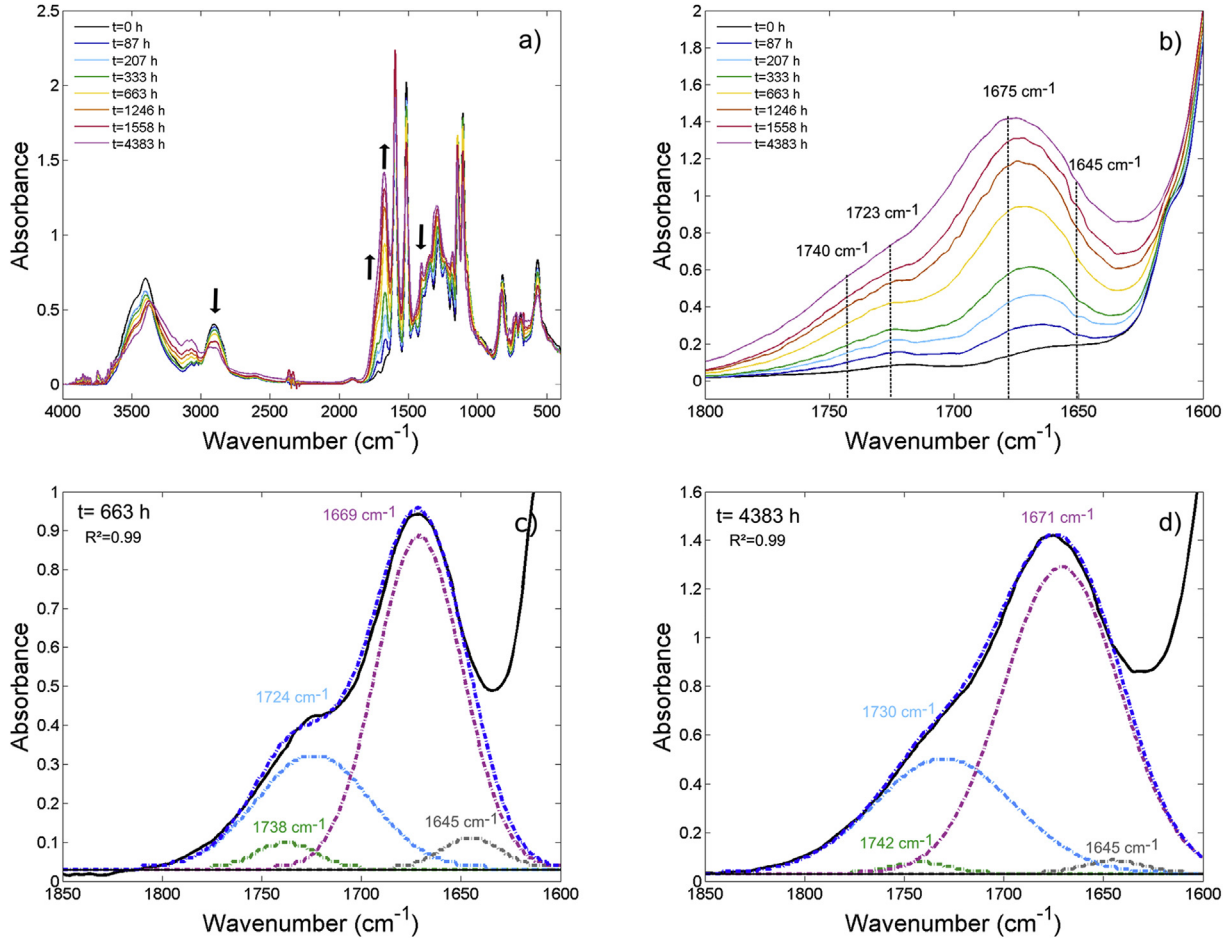

Fig. 7. FTIR spectra for TGMDA-DDS thermally aged under air at 120 °C: full scale spectra (a), carbonyl region (b), deconvolution after 663 (c) and 4383 h (d) of thermal ageing.

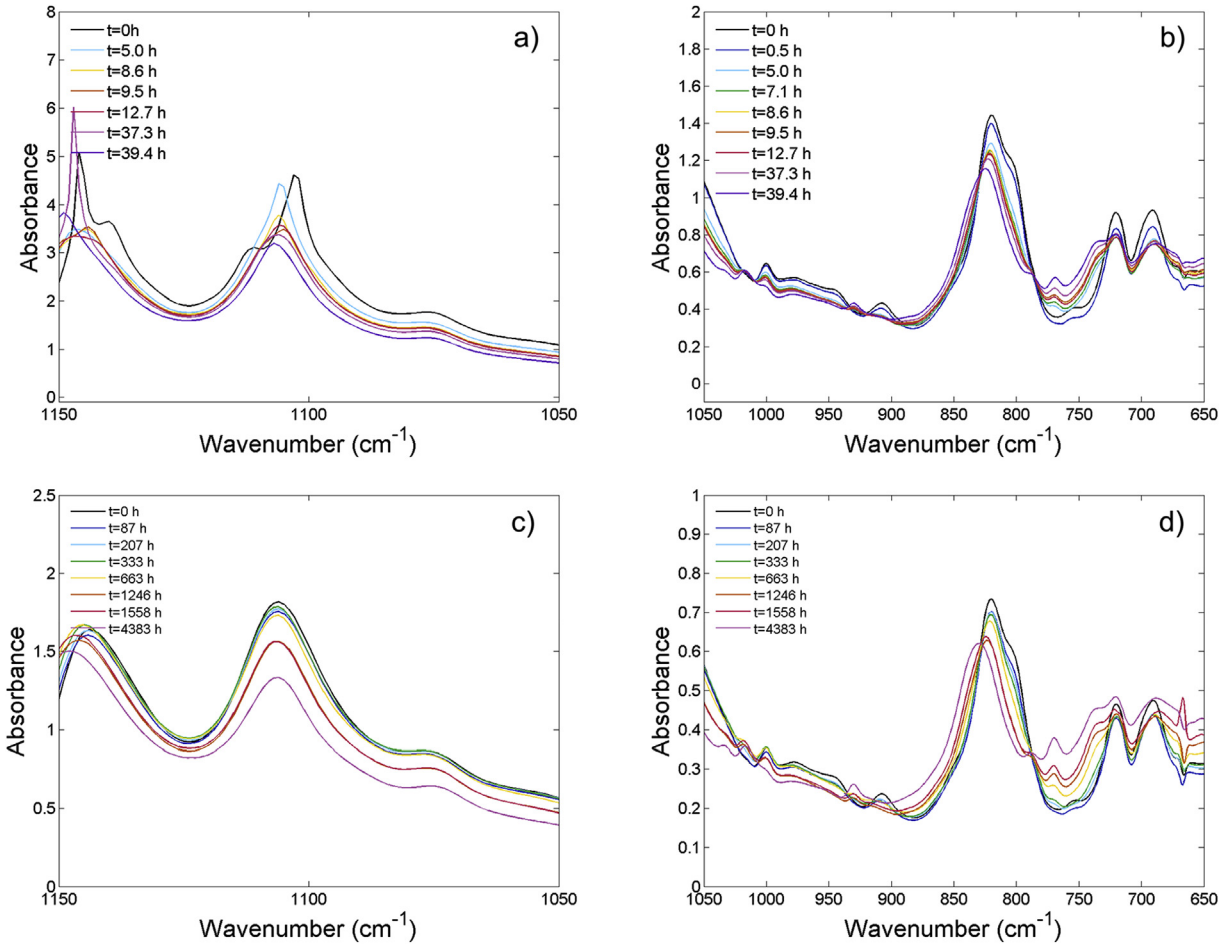

Fig. 8. FTIR spectra for TGMDA-DDS thermally aged under air at 200 (a, b) and 120 °C (c, d) in the C-O (a, c) and =C-H stretching region (b, d).

- imides display a secondary absorbance at 1730 cm^{-1} (see also Appendix) with a 1/3 ratio compared to 1675 cm^{-1} so the absorbance of carbonyls in TGMDA and TGMDA-DDS could be corrected using the following equation:

$$Abs_{corrected} = Abs_{1730} - \frac{1}{3} Abs_{1675} \quad (2)$$

As detailed later, it seems that carboxylic acids are the most probable species. In fact, this uncertainty does not change the main conclusions of the present paper.

Resulting concentrations changes for ageing at 120 °C are plotted in Fig. 13 which calls for the following comments:

- Amide formation is always faster than carbonyls one.
- Thermal oxidation in TGMDA-DDS is always faster than in DGEBA-DDS in terms of amide formation which confirms that CH_2 in α position of TGMDA significantly participate to the oxidation process (and even predominantly compared to CH_2 in α position of DDS nitrogen atoms).
- Whatever the exposure temperature, no induction period is observed identically to similar systems [9–11,30]. The maximal rates for amides and carbonyls formation on DGEBA-DDS and TGMDA-DDS are gathered in Table 2.
- The formation of formates is faster in PKHJ than in DGEBA-DDS, consistently with the higher concentration in -Ar-O-CH_2- in PKHJ (7 mol kg^{-1}) than in DGEBA-DDS (4 mol kg^{-1}).
- In DGEBA DDS, it seems that r_C (for 1730 cm^{-1} absorbance) is slightly higher than r_F (for 1760 cm^{-1} absorbance) but lower than r_A (for 1680 cm^{-1} absorbance). This will be used later for discussing on the relative reactivity of each site.

4. Discussion

The main aim of this section is to propose the most possible mechanisms (i.e. identify the main reactive groups) responsible for the formation of stable oxidation groups which will be used later to establish a scheme to be used for kinetic modeling.

4.1. Possible mechanism of formation of stable products

In DGEBA-DDS, two kinds of carbonyls are generated: formates absorbing at 1765 cm^{-1} and other carbonyl products absorbing at 1720-1730 cm^{-1}. There are for us two possible pathways for explaining their formation:

- one based on the oxidation of methylene in α position of ether leading to a formate and another radical becoming a carboxylic acid (Scheme 1).

- one based on the oxidation of methine C-H in α position of alcohol which will generate primary -CH_2° radical that will give a formate (Scheme 2).

According to Denisov [31], the alkoxy and peroxy in α position of hydroxyl could also decompose and give an aliphatic ketone (Scheme 3). However, such ketones would absorb at 1709 cm^{-1}, that militates against that kind of mechanisms and maybe more

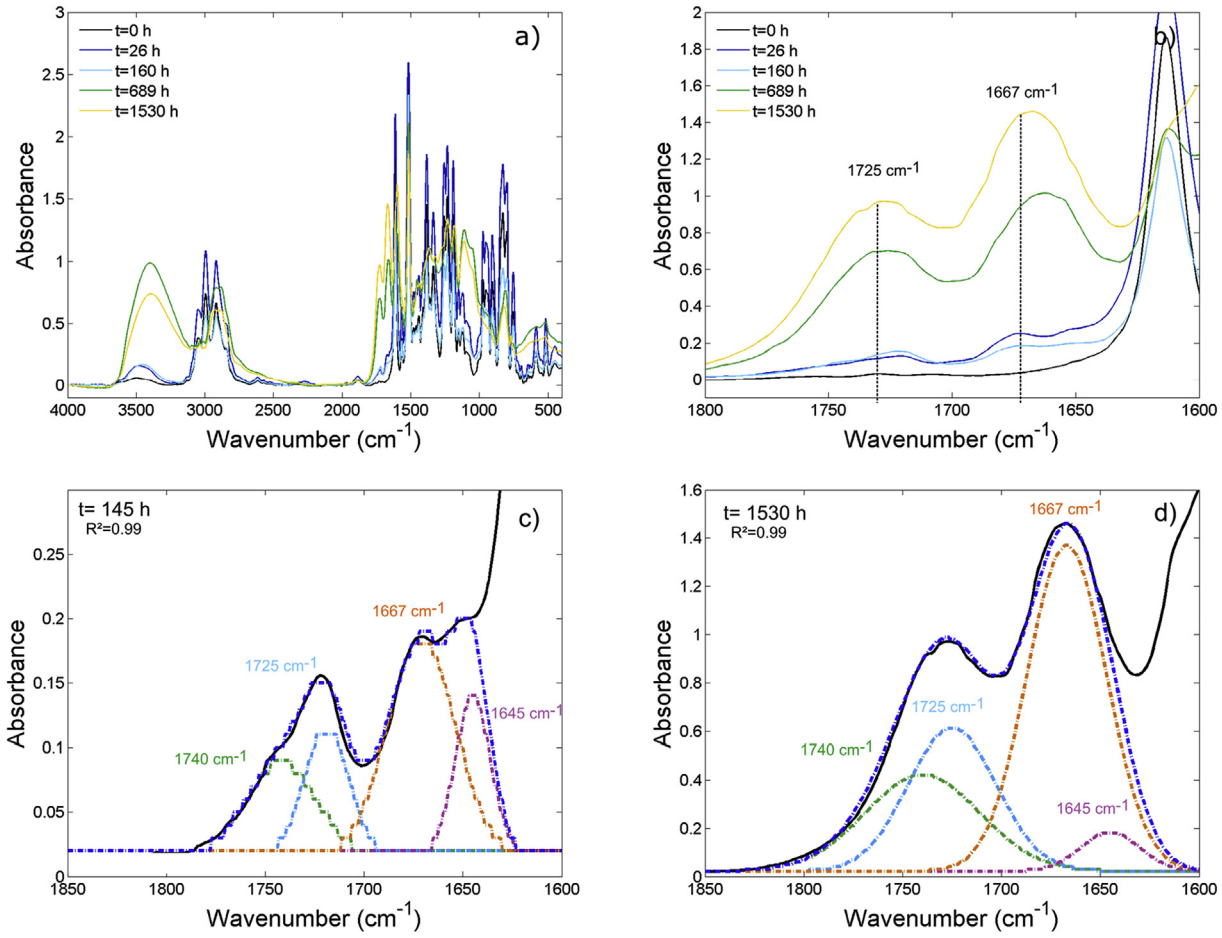

Fig. 9. FTIR spectra of TGMDA monomer thermally aged at 120 °C under air: full scale spectra (a), carbonyl region (b), deconvolution after 145 h (c) and 1530 h (d) of thermal ageing.

generally against the reactivity of the secondary alcohol.

It is however clear that carbonyls actually are carboxylic acids (whatever they are formed from Scheme 1 or Scheme 2) which justifies the choice made for molar absorptivity (see '1.2. TGMDA-DDS' in the 'Result' section).

Amides originate from the oxidation of methylene in α position of nitrogen (Scheme 4a). They give either an amide or an α-hydroxyamide expected to be unstable [32] and leading to a chain scission. The oxidation of >CH-OH could also be considered as illustrated in Scheme 4b.

The formation of the various oxidation products of TGMDA-DDS can also be explained by several pathways: either the radical attack of CH_2 in α position of nitrogens or >CH-OH. At high conversion degrees, it seems also that the amide can easily become an imide, identically to the case of polyamides [33] (Scheme 5) which would explain the shift observed for the 1675 cm^{-1} absorbance. A supplementary level of complexity for modeling the buildup of products absorbing near 1675 cm^{-1} is then expected.

The oxidation of the methylene located between the aromatic rings of TGMDA could also be responsible of the formation of a benzophenone absorbing at 1645 cm^{-1} (Scheme 6). According to Fig. 9, it seems however that this reaction is negligible.

Finally, this short mechanistic discussion does not permit to definitively conclude on the origin of each stable products, since each one can originate from several distinct mechanisms involving either >N-CH_2- or >CH-OH for amides, and -O-CH_2- or >CH-OH for carbonyls. We will hence discuss on the reactivity of each reactive site basing on the available thermochemical and kinetic data existing for comparable model systems.

4.2. On the relative reactivity of each site

Let us recall that the kinetics parameters for the propagation reaction POO° + PH → POOH + P° depend on the Bond Dissociation Energy of the broken C-H (BDE_{C-H}) [34]:

$$log\ k_3^{sPOO^\circ}(30^\circ C) = 16,4 - 0.0478\ \times BDE_{C-H} \quad (3)$$

$$E_3 = 0.55 \times \left(BDE_{(C-H)} - 261,5\right) \quad (4)$$

Here, PH represents C-H in α−position of oxygen, hydroxyl or nitrogen groups. Data for relevant model systems are gathered in Table 3.

The Bond Dissociation Energy of C-H in α of hydroxy in >CH-OH strongly changes with the nature of substituents. The value for isopropanol (which is the model compound the closest to secondary alcohol group in epoxy-diamine and PKHJ) is clearly higher than values of C-H in >N-CH_2- and Ar-O-CH_2- (NB: the same reasons lead us to neglect in a first approach the reactivity of tertiary methyl groups in DGEBA-DDS (since BDE is clearly higher than 400 kJ mol^{-1}).

This suggests that >CH-OH are less likely to undergo a radical attack and militates in favor of mechanisms presented in Schemes 1 and 4a compared to Schemes 2, 3 and 4b. It is consistent with the faster decrease of C-H in Ar-O-CH_2- compared to >CH-OH (Fig. 4). It also brings a supplementary discussion of Fig. 10: 1730 cm^{-1} seems predominating but this peak features a contribution of the 1760 peak. Since species absorbing at 1730 cm^{-1} have a higher molar

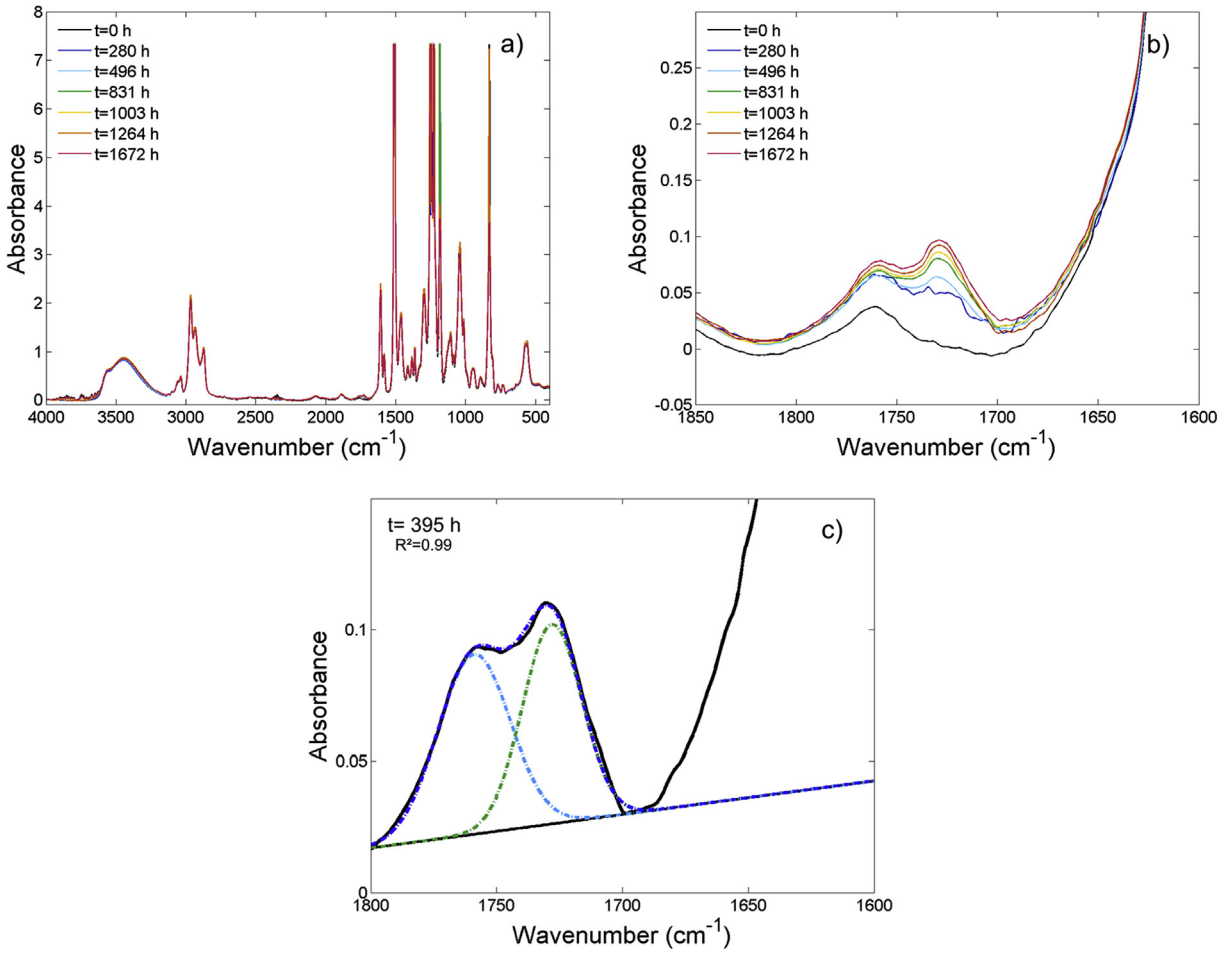

Fig. 10. FTIR spectra of PKHJ thermally aged at 120 °C under air: full scale spectra (a), carbonyl region (b), deconvolution after 395 h (c) and 3591 h (d) of thermal ageing.

absorptivity than 1730 cm^{-1}, it confirms the here above conclusion. However, the full understanding of the relative rates of oxidation product formation (formates, carbonyls and amides in DGEBA-DDS for example – see Fig. 13) and the interplay with them remains an open takes requiring, for example, the use of a co-oxidation kinetic model [38].

The oxidizability of each site can also be expressed by the ratio k_3^2/k_6 (k_3 and k_6 being respectively the rate constants for the $POO^\circ + PH \rightarrow POOH + P^\circ$, and $POO^\circ + POO^\circ \rightarrow$ inactive product). Some possible values are given in Table 4 [39–41] and confirm the lower oxidizability of >CH-OH and of the methylene located between aromatic rings in TGMDA.

Let us note that the above estimations are done for methyl (-CH_3) in α position of amines. In DEGBA-DDS and TGMDA-DDS, the reactive sites are CH_2 expected to be less stable which strengthens our reasoning. In other words, those kinetic and thermochemical data point out that >N-CH_2- and -O-CH_2- play a major role in the degradation course compared to >CH-OH and more surprisingly in a certain extent -Ar-CH_2-Ar-. It remains to better understand the role of the chemical surrounding on the reactivity of methylene in α position of nitrogens to better understand the relative contribution of CH_2 in α position of the nitrogen hold by TGMDA or DDS.

4.3. On the origin of amides and the role of DDS hardener

According to Table 3, the ratio of rate of amides formation in TGMDA-DDS over rate of amides formation in DGEBA-DDS decreases from about 35 at 80 °C to 3.5 at 200 °C. Let us recall that those rates are linked to the concentration in reactive sites by:

$$r_{ox} = \left(\frac{k_3^2}{k_6}\right)[PH]^2 \quad (5)$$

where k_3 and k_6 are respectively the rate constants for propagation ($POO^\circ + PH \rightarrow POOH + P^\circ$) and termination ($POO^\circ + POO^\circ \rightarrow$ inactive products), and [PH] is the concentration in reactive sites that can be estimated from:

$$[PH] = \frac{Number\ of\ oxidizable\ sites}{M_{UCR}} \quad (6)$$

M_{UCR} being the molar mass of the repetitive constitutive unit (i.e. 928 g mol^{-1} for DGEBA DDS and 670 g mol^{-1} for TGMDA-DDS). It leads to:

- $[PH]_{\alpha\text{-}N} = 4.3$ mol kg^{-1} in DGEBA-DDS
- $[PH]_{\alpha\text{-}N} = 12$ mol kg^{-1} in TGMDA-DDS (with $[PH]_{\alpha\text{-}N} = 6$ mol kg^{-1} for CH_2 in α position of the nitrogen atom hold by TGMDA and $[PH]_{\alpha\text{-}N} = 6$ mol kg^{-1} for CH_2 in α position of the nitrogen atom hold by DDS).

In other words, if all $CH_{2\alpha\text{-}N}$ would have the same reactivity, the ratio $(r_{amide})_{TGMDA\text{-}DDS}/(r_{amide})_{DGEBA\text{-}DDS}$ should be close to $(12/4.3)^2$–10 irrespectively of the temperature. However, this ratio is clearly higher than 10 at 120 °C meaning that CH_2 in α position of nitrogen hold by TGMDA are much more reactive than CH_2 in α

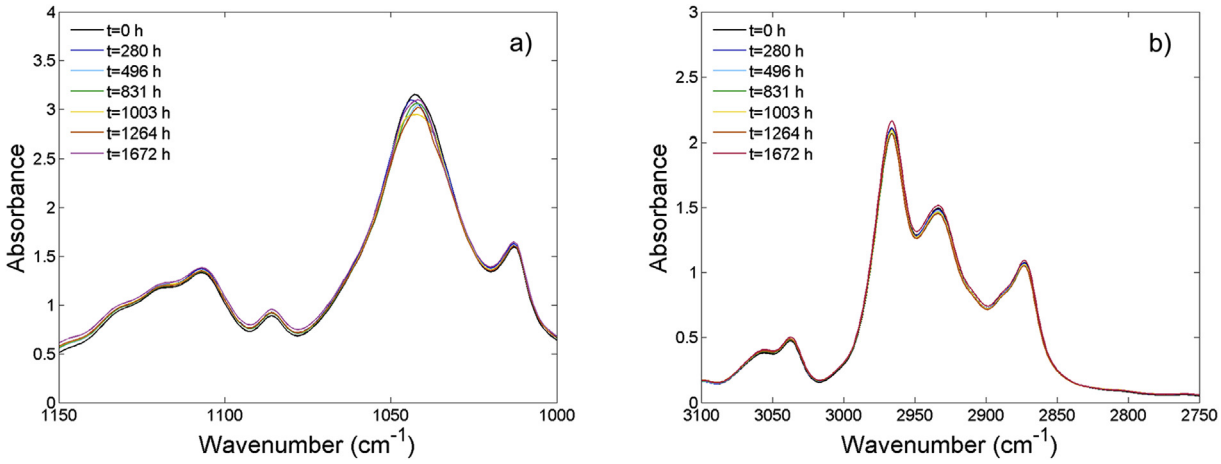

Fig. 11. FTIR spectra of PKHJ thermally aged at 120 °C under air in the region of C-O (a) and C-H stretching (b).

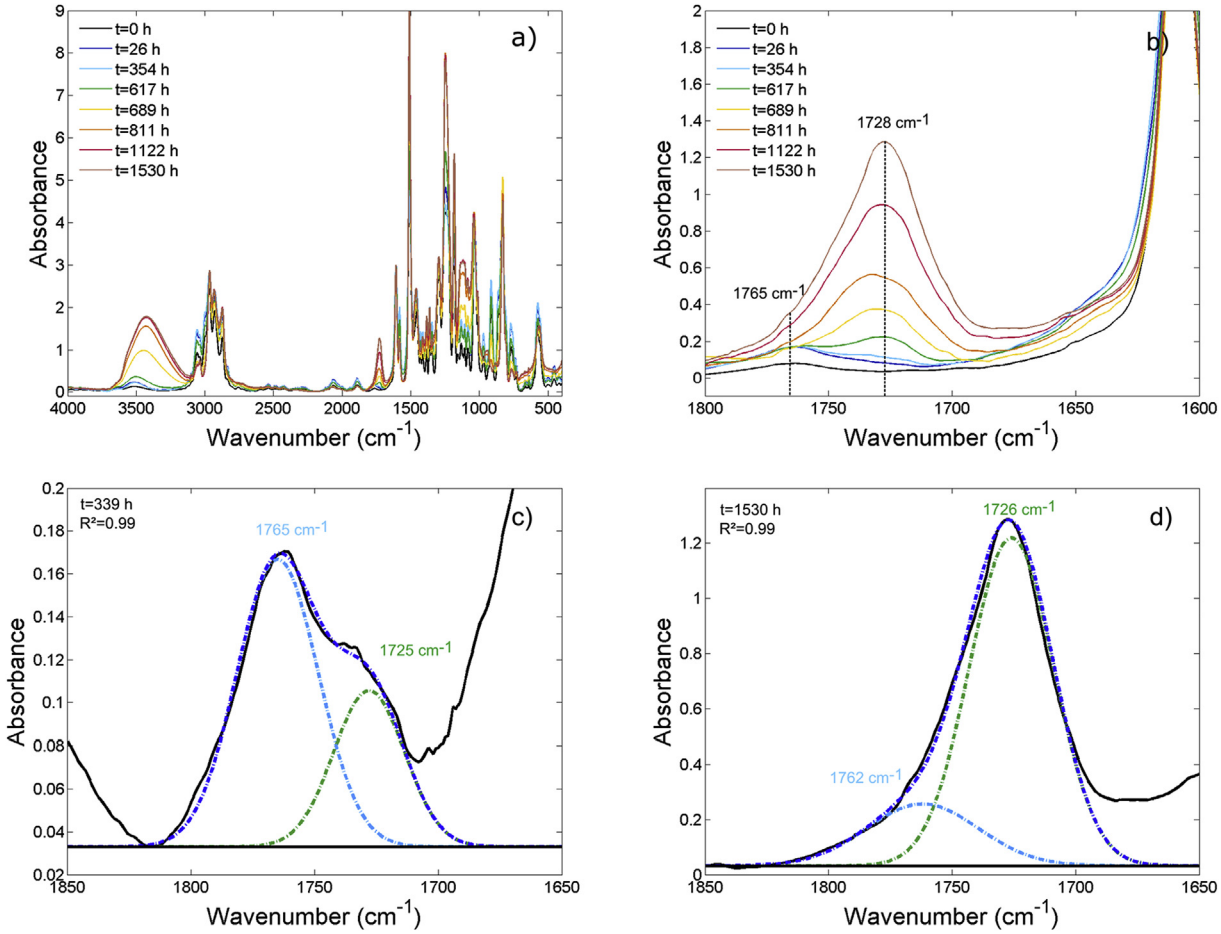

Fig. 12. FTIR spectra of DGEBA thermally aged at 120 °C under air: full scale spectra (a), carbonyl region (b), deconvolution after 335 h (c) and 1530 h (d) of thermal ageing.

position of DDS (this difference decreasing with temperature). This seems confirmed by the comparison of amide formation in TGMDA-DDS and TGMDA at 120 °C: $r_{amide} = 6.7\times10^{-7}\,mol\,l^{-1}\,s^{-1}$ with $[PH]_{\alpha\text{-}N} = 9\,mol\,l^{-1}$ in TGMDA versus $r_{amide} = 5.6\times10^{-7}\,mol\,l^{-1}\,s^{-1}$ with $[PH]_{\alpha\text{-}N} = 12\,mol\,l^{-1}$ in TGMDA-DDS. It involves that $10^7\times r_{amide}/[PH]^2 = 0.084$ in TGMDA versus 0.039 in TGMDA-DDS pointing out the highest reactive of methylenes vicinal to N hold by TGMDA compared to N hold by DDS.

According to Eichler et al. [42], the presence of attractive SO_2 group induces a decrease of the electronic density on DDS nitrogen atom (for example compared to DiaminoDiphenylMethane). This explains for example the difference in reactivity towards epoxies and the matter that the polymerization onset occurs at lower temperature for epoxies cured with DDM than with DDS [43].

In other words, the DDS effect induces:

- either a higher Bond Dissociation Energy (than reported in Table 3) and then a slower propagation kinetics. Interestingly, it can be noted a higher Bond Dissociation Energy means a higher activation energy for propagation (Eq. (4)) so that the reaction

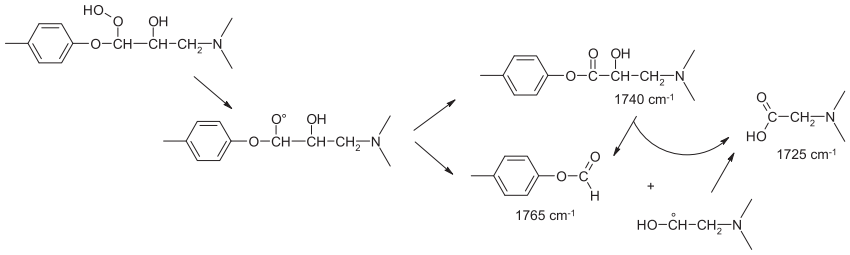

Scheme 1. Possible oxidation mechanism of -Ar-O-CH_2- group in DGEBA-DDS.

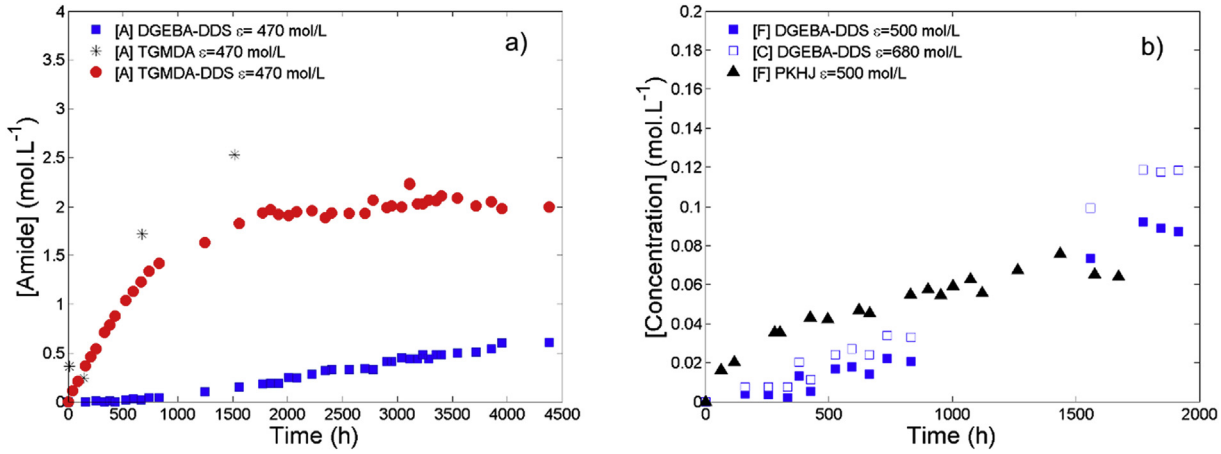

Fig. 13. Changes in amides [A] and carbonyls [C] for systems under study thermally aged under air at 120 °C.

Table 2
Maximal rates for amides and carbonyls formations at 80, 120 and 200 °C under air.

Systems	DGEBA-DDS		TGMDA-DDS	
Maximal rate of amides formation (mol l^{-1} s^{-1})				
r_{ox} 80 °C	4.69×10^{-10}		1.87×10^{-8}	
r_{ox} 120 °C	3.75×10^{-8}		5.61×10^{-7}	
r_{ox} 200 °C	1.20×10^{-5}		4.15×10^{-5}	
Maximal rate for carbonyls formation (mol l^{-1} s^{-1})				
		*[C]corr		*[C]corr
r_{ox} 80 °C	3.36×10^{-10}	2.22×10^{-10}	5.56×10^{-9}	1.94×10^{-9}
r_{ox} 120 °C	2.22×10^{-8}	1.38×10^{-8}	1.10×10^{-7}	3.28×10^{-8}
r_{ox} 200 °C	9.42×10^{-6}	3.55×10^{-6}	1.16×10^{-5}	2.83×10^{-6}

* The corrected concentration is obtained according to the Equation (2).

on CH_2 in α position of DDS becomes possible at higher temperatures consistently with the decrease of the ratio $(r_{amide})_{TGMDA\text{-}DDS}/(r_{amide})_{DGEBA\text{-}DDS}$.

- or a « stabilization » of the hydroperoxides but in principle, the stability of hydroperoxides does not influence the maximal rate of oxidation (according to Eq. (5))

Finding the right explanation, together with refining the data given in Tables 3 and 4, remains open and requires for us the need of quantum calculations [44,45] to get more quantitative explanations and more precise estimation of Bond Dissociation Energies at the ageing temperature (instead of 298 K as usually given in monographs).

5. Conclusions

The embrittlement of thermally oxidized epoxy-diamine networks is linked to the disappearance of the hydroxypropylether function, which is the main reactive group in DGEBA-DDS and possibly in TGMDA-DDS. In this work, we tentatively identified the main reactive sites in those epoxy systems by studying their thermal degradation with the help of comparison with some model compounds displaying some structural similarities and quantitative arguments (assessment of rates of formation of stable products, estimated values of Bond Dissociation Energies). It was concluded that:

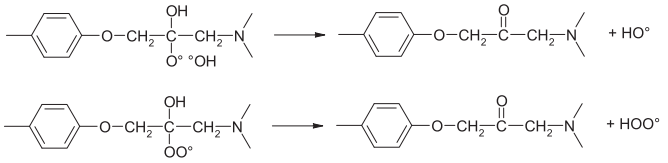

Scheme 3. Possible pathways for the formation of aliphatic ketones.

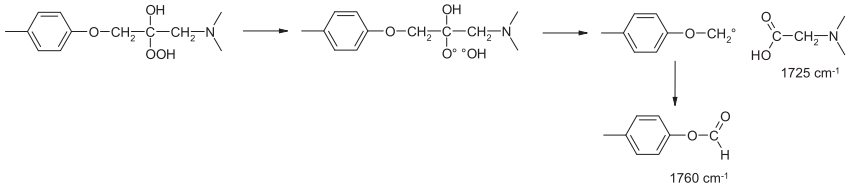

Scheme 2. Possible oxidation mechanism of >CH-OH group in DGEBA-DDS.

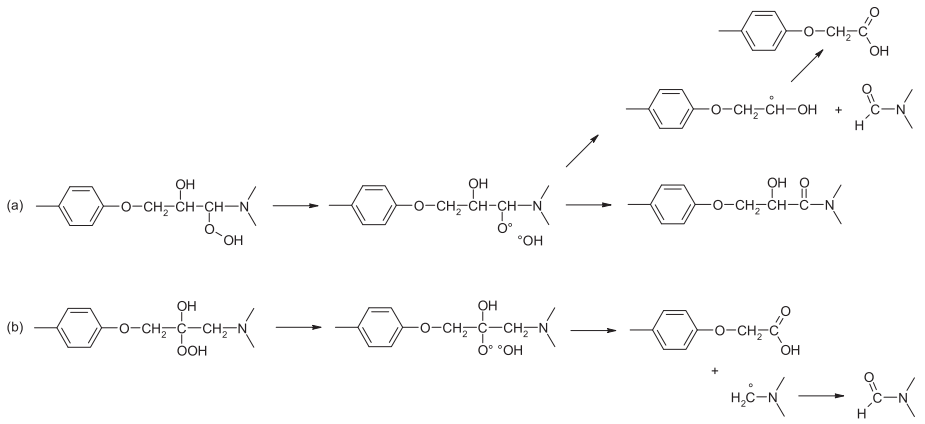

Scheme 4. Possible pathways of amide by-products from oxidation of methylenes in α position of nitrogen (a) or β one (b).

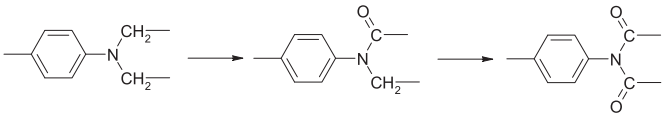

Scheme 5. Formation of imides in TGMDA and TGMDA-DDS.

Scheme 6. Possible mechanism for benzophenone formation in TGMDA-DDS.

- the CH_2 in α position of ether is more reactive than >CH-OH in DGEBA-DDS and leads to a formate. The CH_2 in α position of DDS is expected to generate an amide, and can also be involved either at relatively long times (at low temperature) and more significantly at higher temperatures.

Table 4
Oxidizability of some model compounds.

	$k_3/(2k_6)^{1/2}$ (120 °C)	$k_3/(2k_6)^{1/2}$ (200 °C)
$PhNMe_2$	0.152	0.360
	0.105	0.313
Ar-CH_2-Ar	0.008	0.061
Me_2CHOH	0.006	0.086

- the CH_2 in α position of nitrogen hold by TGMDA seems to be the main reactive site in TGMDA-DDS and generates an amide. It seems to be much more reactive (at low temperature) than CH_2 in α position of DDS.

In the past, the main attempts to model the kinetics of epoxies thermal oxidation assumed the unicity of reactive sites i.e. that the reactivity of all C-H present in the hydroxypropylether is ruled by a

Table 3
Bond Dissociation Energies and kinetic parameters for propagation reaction in model compounds [35–37]. * denotes the model compound matching the better with epoxy-diamine systems under investigation. (NB: a supplementary discussion of those values is given in Appendix 2).

		BDE (kJ mol^{-1})	E_3 (kJ mol^{-1})	k_3(120 °C) (l mol^{-1} s^{-1})	k_3(200 °C) (l mol^{-1} s^{-1})
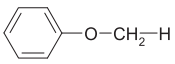	*	385	68	4.8	160.0
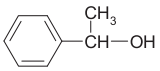		356	52	27.3	400.4
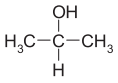	*	390.5	71	3.4	134.4
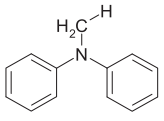		379.5	65	6.6	190.4
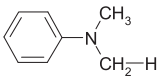		383.7	67	5.2	166.7
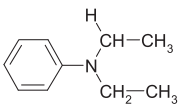	*	383.2	67	5.3	169.4
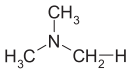		376.6	63	7.9	208.7

unique set of rate constants. It seems now clear that only a co-oxidation kinetic model (mixing various kinds of reactive units) can describe the degradation of epoxy-diamine networks [36]. The adjustment of the numerous rate constants requires a deeper investigation which goes out of the scope of the present paper. However, the study of model compounds (as presented in this work) will be helpful to estimate most of them as illustrated in a promising preliminary work [46].

Acknowledgements

Agence Nationale de la Recherche et de la Technologie is gratefully acknowledged for having granted this study (Cifre N° 2015-0424).

APPENDIX 1

Some of the characteristic absorptions reported in Table 2 were checked from spectra performed on model compounds (see Fig. 14):

- Phenyl acetate (CAS 122-79-2 - ref 30311-1 ML from Sigma Aldrich)
- Phenyl formate (CAS 1864-94-4 – ref 06556-5 ML from Sigma Aldrich)
- 1-Phenyl-2,6-Piperazinedione (ref PH007876-25 MG from Sigma Aldrich)

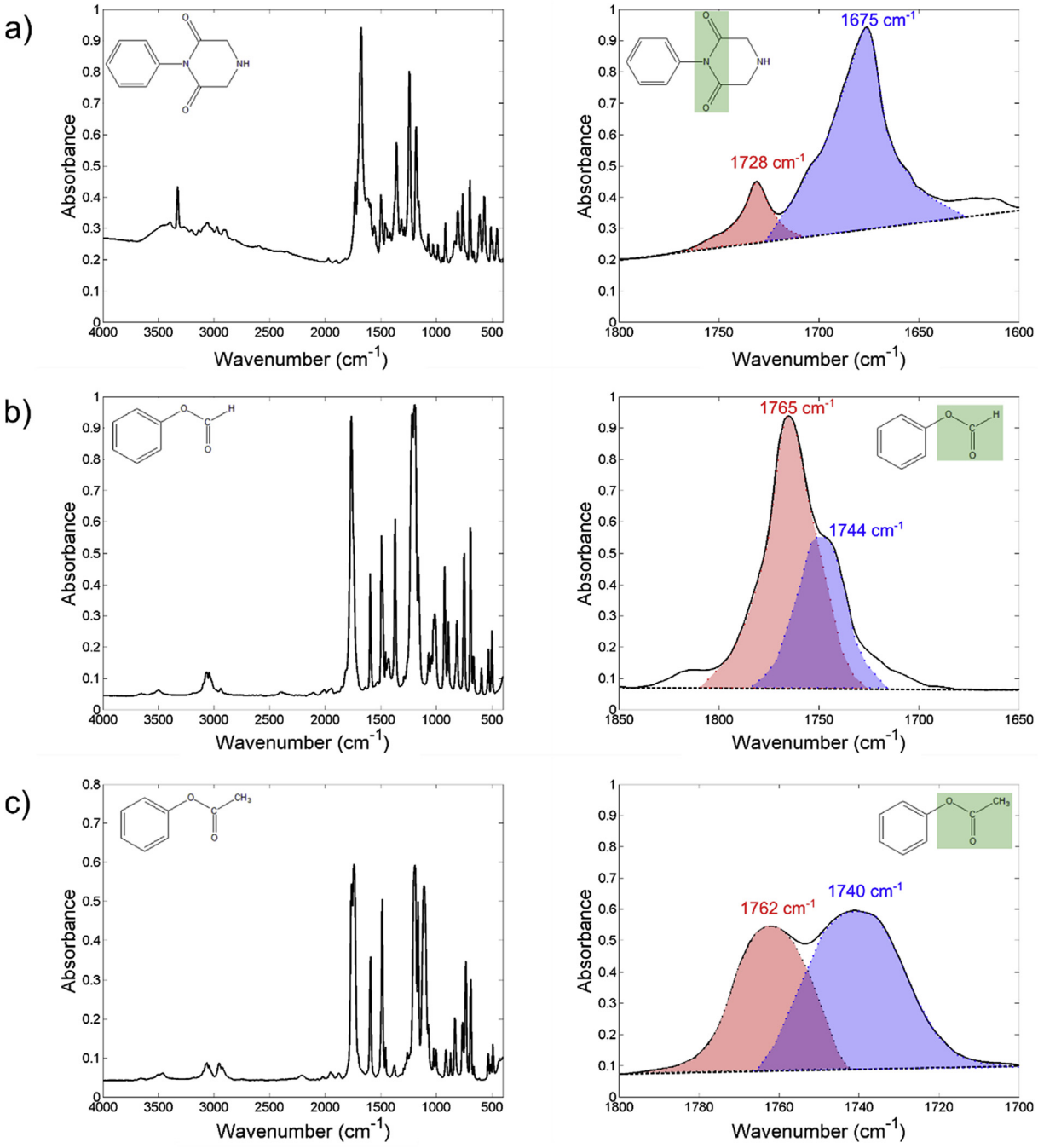

Fig. 14. FTIR spectra of model compounds: Imide (a), phenyl formate (b) and phenyl acetate (c).

APPENDIX 2

The issue of the Bond dissociation Energy values used for discussing our mechanisms is not trivial:

- Firstly, values are given for model compounds matching more or less the reactive groups presents in epoxies.
- Secondly, they are usually given at 298 K and there is no simple maneer to extrapolate them in the ageing conditions under study.
- Thirdly, there are conformational effects in networks which can change the BDE value compared to simple molecules.
- Last, there is a certain scattering due to the multiple origin of values.

For example:

- For C-H in triethylamine, the CRC Handbook reports five values equal to 355.6, 381, 379.5, 372.4 and 381.6 [47] which is well in line (apart one value) with Table 3.
- For C-H in α position of alcohol, situation is more intricate: the CRC Handbook reports four values scattered from 373.6 to 390 kJ mol^{-1} meanwhile a significantly higher value (395 kJ mol^{-1}) can be found in Ref. [48].
- For anisole (or better phenetole), data are particulary hard to find. The CRC Handbook does not feature their values. We only noted that C-H ethers at viciny of ethers are relatively oxidizable (ref [34] reports for example a 370 kJ mol^{-1} for isopropyl phenyl ether).

To conclude:

- We chose data coming from the same monograph ("Oxidation and Antioxidants in Organic Chemistry and Biology" [35–37]) because primary references involve the same main author (E. Denisov) so that we expect the experiments were done in reproducible conditions.
- We stress on the fact that those thermochemical data must be refined in the future by DFT calculations taking into account the electroattractive and hindrance effects and any other difference between model systems and cured networks in their ageing conditions.
- At last, for example in the case of the C-H position in α-position of ethers, the comparison for example with oxidation of DGEBA (monomer) or PKHJ monomer helped us to choose the most reactive sites in DGEBA-DDS.

References

[1] S. Terekhina, M. Mille, B. Fayolle, X. Colin, Oxidation induced changes in viscoelastic properties of a thermostable epoxy matrix, Polym. Sci. 55 (2013) 614–624. https://doi.org/10.1134/S0965545X13090058.

[2] E. Ernault, E. Richaud, B. Fayolle, Thermal-oxidation of epoxy/amine followed by glass transition temperature changes, Polym. Degrad. Stabil. 138 (2017) 82–90. https://doi.org/10.1016/j.polymdegradstab.2017.02.013.

[3] X. Buch, M.E.R. Shanahan, Thermal and thermo-oxidative ageing of an epoxy adhesive, Polym. Degrad. Stabil. 68 (2000) 403–411. https://doi.org/10.1016/S0141-3910(00)00028-8.

[4] N.H. Giron, M.C. Celina, High temperature polymer degradation: rapid IR flow-through method for volatile quantification, Polym. Degrad. Stabil. 145 (2017) 93–101. https://doi.org/10.1016/j.polymdegradstab.2017.05.013.

[5] X. Colin, A. Mavel, C. Marais, J. Verdu. Interaction between cracking and oxidation in organic matrix composites, J. Compos. Mater. 39 (2005) 1371–1389. https://doi.org/10.1177/0021998305050430.

[6] B.J. Anderson, Thermal stability of high temperature epoxy adhesives by thermogravimetric and adhesive strength measurements, Polym. Degrad. Stabil. 96 (2011) 1874–1881. https://doi.org/10.1016/j.polymdegradstab.2011.07.010.

[7] J. Delozanne, N. Desgardin, M. Coulaud, N. Cuvillier, E. Richaud. Failure of epoxies bonded assemblies: comparison of thermal and humid ageing. J. Adhes. In Press. doi.org/10.1080/00218464.2018.1547198.

[8] T. Kamon, H. Furukawa, Curing mechanisms and mechanical properties of cured epoxy resins, in: K. Dušek (Ed.), Epoxy Resins and Composites IV, vol. 80, 1986, pp. 173–202. Advances in Polymer Science.

[9] E. Ernault, E. Richaud, B. Fayolle, Thermal oxidation of epoxies: influence of diamine hardener, Polym. Degrad. Stabil. 134 (2016) 76–86. https://doi.org/10.1016/j.polymdegradstab.2016.09.030.

[10] Y. Zahra, F. Djouani, B. Fayolle, M. Kuntz, J. Verdu, Thermo-oxidative aging of epoxy coating systems, Prog. Org. Coating 77 (2014) 380–387. https://doi.org/10.1016/j.porgcoat.2013.10.011.

[11] C. Galant, B. Fayolle, M. Kuntz, J. Verdu, Thermal and radio-oxidation of epoxy coatings, Prog. Org. Coating 69 (2010) 322–329. https://doi.org/10.1016/j.porgcoat.2010.07.005.

[12] S. Cukierman, J.-L. Halary, L. Monnerie, Molecular analysis of the viscoelastic properties of epoxy networks as deduced from the study of model systems, J. Non-Cryst. Solids 131–133 (1991) 898–905. https://doi.org/10.1016/0022-3093(91)90700-G.

[13] V. Bellenger, J. Verdu, Effect of structure on glass transition temperature of amine crosslinked epoxies, J. Polym. Sci. B Polym. Phys. 25 (1987) 1219–1234. https://doi.org/10.1002/polb.1987.090250604.

[14] P. Musto, G. Ragosta, P. Russo, L. Mascia, Thermal-Oxidative degradation of epoxy and epoxy bismaleimide networks: kinetics and mechanism, Macromol. Chem. Phys. 202 (2001) 3445–3458. https://doi.org/10.1002/1521-3935(20011201)202:18<3445::AID-MACP3445>3.0.CO;2-N.

[15] P. Musto, Two-dimensional FTIR spectroscopy studies on the thermal-oxidative degradation of epoxy and Epoxy–Bis(maleimide) networks, Macromolecules 36 (2003) 3210–3221, https://doi.org/10.1021/ma0214815.

[16] S.V. Levchik, G. Camino, M.P. Luda, L. Costa, B. Costes, Y. Henry, G. Muller, E. Morel, Mechanistic study of thermal behaviour and combustion performance of epoxy resins. II. TGDDM/DDS system, Polym. Degrad. Stabil. 48 (1995) 359–370. https://doi.org/10.1016/0141-3910(95)00084-Y.

[17] P. Musto, M. Abbate, M. Pannico, G. Scarinzi, G. Ragosta, Improving the photo-oxidative stability of epoxy resins by use of functional POSS additives: a spectroscopic, mechanical and morphological study, Polymer 53 (2012) 5016–5036. https://doi.org/10.1016/j.polymer.2012.08.063.

[18] V. Bellenger, J. Verdu, Structure-photooxidative stability relationship of amine-crosslinked epoxies, Polym. Photochem. 5 (1984) 295–311. https://doi.org/10.1016/0144-2880(84)90039-3.

[19] J. Decelle, N. Huet, V. Bellenger, Oxidation induced shrinkage for thermally aged epoxy networks, Polym. Degrad. Stabil. 81 (2003) 239–248. https://doi.org/10.1016/S0141-3910(03)00094-6.

[20] X. Colin, C. Marais, J. Verdu, Kinetic modelling and simulation of gravimetric curves: application to the oxidation of bismaleimide and epoxy resins, Polym. Degrad. Stabil. 78 (2002) 545–553. https://doi.org/10.1016/S0141-3910(02)00230-6.

[21] E. Ernault, J. Dirrenberger, E. Richaud, B. Fayolle, Prediction of stress induced by heterogeneous oxidation: case of epoxy/amine networks, Polym. Degrad. Stabil. 162 (2019) 112–121. https://doi.org/10.1016/j.polymdegradstab.2019.02.019.

[22] A. Quintana, M.C. Celina, Overview of DLO modeling and approaches to predict heterogeneous oxidative polymer degradation, Polym. Degrad. Stabil. 149 (2018) 173–191. https://doi.org/10.1016/j.polymdegradstab.2017.11.014.

[23] J. Lacoste, D. Vaillant, D.J. Carlsson, Gamma-, photo-, and thermally-initiated oxidation of isotactic polypropylene, J. Polym. Sci.: Polym. Chem. 31 (1993) 715–722. https://doi.org/10.1002/pola.1993.080310316.

[24] https://www.sigmaaldrich.com/catalog/product/aldrich/241989?lang=fr&region=FR.

[25] http://www.spectroscopyonline.com/alcohols-rest-story.

[26] A. Rivaton, L. Moreau, J.-L. Gardette, Photo-oxidation of phenoxy resins at long and short wavelengths—II. Mechanisms of formation of photoproducts, Polym. Degrad. Stabil. 58 (1997) 333–339. https://doi.org/10.1016/S0141-3910(97)00088-8.

[27] A. Rivaton, B. Mailhot, J. Soulestin, H. Varghese, J.L. Gardette, Comparison of the photochemical and thermal degradation of bisphenol-A polycarbonate and trimethylcyclohexane–polycarbonate, Polym. Degrad. Stabil. 75 (2002) 17–33. https://doi.org/10.1016/S0141-3910(01)00201-4.

[28] B. Mailhot, S. Morlat-Thérias, M. Ouahioune, J.-L. Gardette, Study of the degradation of an epoxy/amine resin, 1, Macromol. Chem. Phys. 206 (2005) 575–584. https://doi.org/10.1002/macp.200400395.

[29] M. Gardette, A. Perthue, J.-L. Gardette, T. Janecska, E. Földes, B. Pukánszky, S. Therias, Photo- and thermal-oxidation of polyethylene: comparison of mechanisms and influence of unsaturation content, Polym. Degrad. Stabil. 98 (2013) 2383–2390. https://doi.org/10.1016/j.polymdegradstab.2013.07.017.

[30] C. Galant, B. Fayolle, M. Kuntz, J. Verdu, Thermal and radio-oxidation of epoxy coatings, Prog. Org. Coating 69 (2010) 322–329. https://doi.org/10.1016/j.porgcoat.2010.07.005.

[31] E.T. Denisov, I.B. Afanas'ev, Oxidation and Antioxidants in Organic Chemistry and Biology, Taylor & Francis Group, 2005. Chap 7. Oxidation of Alcohols and Ethers.

[32] J. Lemaire, R. Arnaud, J.-L. Gardette, Low temperature thermo-oxidation of thermoplastics in the solid state, Polym. Degrad. Stabil. 33 (1991) 277–294. https://doi.org/10.1016/0141-3910(91)90021-I.

[33] E. Richaud, O. Okamba Diogo, B. Fayolle, J. Verdu, J. Guilment, F. Fernagut,

Review: auto-oxidation of aliphatic polyamides, Polym. Degrad. Stabil. 98 (2013) 1929–1939. https://doi.org/10.1016/j.polymdegradstab.2013.04.012.
[34] S. Korcek, J.H.B. Chenier, J.A. Howard, K.U. Ingold, Absolute rate constants for hydrocarbon autoxidation. XXI. Activation Energies for propagation and the correlation of propagation rate constants with carbon–hydrogen Bond strengths, Rev. Can. Chim. 50 (1972) 2285–2297. https://doi.org/10.1139/v72-365.
[35] E.T. Denisov, I.B. Afanas'ev, Oxidation and Antioxidants in Organic Chemistry and Biology, Taylor & Francis Group, 2005. Chap 7. Oxidation of Alcohols and Ethers. Table 7.1.
[36] E.T. Denisov, I.B. Afanas'ev, Oxidation and Antioxidants in Organic Chemistry and Biology, Taylor & Francis Group, 2005. Chap 7. Oxidation of Alcohols and Ethers. Table 7.11.
[37] E.T. Denisov, I.B. Afanas'ev, Oxidation and Antioxidants in Organic Chemistry and Biology, Taylor & Francis Group, 2005. Chap 9. Oxidation of Amines, Amides, and Esters. Table 9.1.
[38] E. Richaud, B. Fayolle, J. Verdu, J. Rychlý, Co-oxidation kinetic model for the thermal oxidation of polyethylene-unsaturated substrate systems, Polym. Degrad. Stabil. 98 (2013) 1081–1088. https://doi.org/10.1016/j.polymdegradstab.2013.01.008.
[39] E.T. Denisov, I.B. Afanas'ev, Oxidation and Antioxidants in Organic Chemistry and Biology, Taylor & Francis Group, 2005. Chap. 9. Oxidation of Amines, Amides, and Esters. Table 9.2.
[40] E.T. Denisov, I.B. Afanas'ev, Oxidation and Antioxidants in Organic Chemistry and Biology, Taylor & Francis Group, 2005. Chain Mechanism of Liquid-Phase Oxidation of Hydrocarbons.Table 2.1.
[41] E.T. Denisov, I.B. Afanas'ev, Oxidation and Antioxidants in Organic Chemistry and Biology, Taylor & Francis Group, 2005. Chap 7. Oxidation of Alcohols and Ethers. Table 7.2.
[42] V.J. Eichler, J. Mleziva, Studium der Reaktivität von aromatischen Diaminen mit Epoxidharzen, Angew. Makromol. Chem. 19 (1971) 31–55. https://doi.org/10.1002/apmc.1971.050190103.
[43] M.F. Mustafa, W.D. Cook, T.L. Schiller, H.M. Siddiqi, Curing behavior and thermal properties of TGDDM copolymerized with a new pyridine-containing diamine and with DDM or DDS, Thermochim. Acta 575 (2014) 21–28. https://doi.org/10.1016/j.tca.2013.09.018.
[44] D. Bertin, M. Leblanc, S.R.A. Marque, D. Siri, Polypropylene degradation: theoretical and experimental investigations, Polym. Degrad. Stabil. 95 (2010) 782–791. https://doi.org/10.1016/j.polymdegradstab.2010.02.006.
[45] D. Bertin, S. Grimaldi, M. Leblanc, S.R.A. Marque, D. Siri, P. Tordo, A DFT study of the hydrogen atom abstraction from 2,4,6-trimethylheptane: a model of peroxidic degradation for syndio polypropylene, J. Mol. Struct. (Theochem) 811 (2007) 255–266. https://doi.org/10.1016/j.theochem.2007.03.008.
[46] J. Delozanne, Durabilité des époxys – Application au collage structural aéronautique, PhD thesis, Arts et Métiers ParisTech, 2018.
[47] Yu-Ran Luo, Handbook of Bond Dissociation Energies in Organic Compounds || Tabulated BDEs of C–H Bonds, 2002, https://doi.org/10.1201/9781420039863.ch3.
[48] V.B. Oyeyemi, J.A. Keith, E.A. Carter, Trends in Bond dissociation Energies of alcohols and aldehydes computed with multireference averaged coupled-pair functional theory, J. Phys. Chem. A 118 (2014) 3039–3050. https://doi.org/10.1021/jp501636r.